

1 A Practical Tool for Predicting the Minimum Ignition Energy of 2 Organic Dusts

3 Sabrina Copelli, Martina S. Scotton, Marco Barozzi, Marco Derudi, and Renato Rota*




Cite This: <https://doi.org/10.1021/acs.iecr.1c00309>



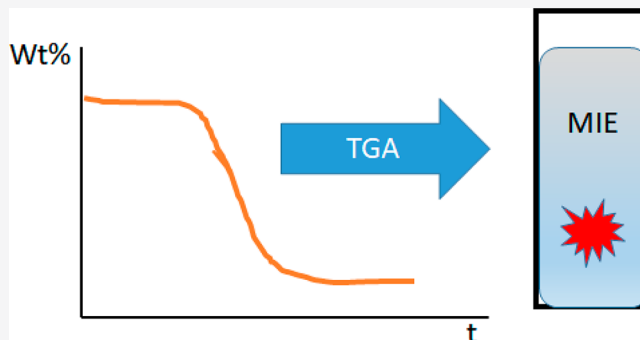
Read Online

ACCESS |

 Metrics & More

 Article Recommendations

4 **ABSTRACT:** In the last decades, protection and prevention in the
5 workplace has assumed great relevance. In this context, organic
6 dust explosions represent one of the major risks. Within this frame,
7 the minimum ignition energy (MIE) of a dust occupies a
8 fundamental role for the assessment of the explosibility hazard.
9 At present, the measurement of the MIE is performed using the
10 standard Hartmann apparatus. This approach involves some
11 practical limitations, mainly related to the testing times and
12 costs. This work is focused on developing both a mathematical
13 model capable of describing the main phenomena leading to the
14 ignition of an organic dust inside a Hartmann tube and a simpler
15 procedure for the estimation of the MIE. Such an approach relies
16 on the use of accessible physicochemical properties and simple
17 thermogravimetric analysis (TGA) experiments, coupled with a particle size analysis capable of providing a mean characteristic
18 diameter of the dust. The proposed procedure has been validated by comparison with literature experimental data of minimum
19 ignition energy of several organic dusts, showing a fair agreement among experimental results and model predictions.



1. INTRODUCTION

20 Industrial safety has been always a subject of great concern,
21 especially in recent years, because of the relatively high number
22 of industrial accidents and negative associated consequences.
23 In 2020, the number of major accidents that occurred in
24 industrial facilities increased globally, especially because of the
25 post-lockdown refurbishment of plants.¹ According to a report
26 published by the Industrial Global Union² in India, there was
27 an average of one accident and one death per alternate day
28 only in the month of May 2020 and, among the months of
29 January and August 2020, there were at least 25 serious
30 industrial accidents, which caused over than 120 deaths. There
31 were also reports of similar accidents in the industrial facilities
32 restarted up in other parts of Asia, as well as Italy, Turkey, and
33 the United States. Also, according to CCPS,³ it is well-known
34 that process safety accidents occur five times more frequently
35 during start-up and shut-down operations than during normal
36 activities. Moreover, industrial accidents are not only related to
37 the re-startup of plants after a prolonged stop, but they can be
38 also connected to normal operations or storage of potentially
39 dangerous materials in warehouses. This is what happened in
40 Beirut on August 2020, where a large amount of ammonium
41 nitrate stored in a port warehouse exploded, causing at least
42 203 deaths and 6500 injuries.⁴ With regard to dust explosions,
43 in 2019, 87% of the global fatalities recorded occurred because
44 of dust explosions and, of this percentage, up to 65% were due
45 to organic dusts such as wood and food products;⁵

furthermore, in the first semester of 2020, 26 dust explosions
occurred worldwide, and 80% of them were caused by organic
dusts.⁶ Such data simply confirm the importance of increasing
the safety of plants managing explosive dusts through the
implementation of risk assessment procedures using either
traditional methods, such as HazOp, FTA, FMEA, or
innovative ones, such as ROA-ISD,^{7,8} which is specifically
tailored for organic dust explosions.

Regardless of the method used for risk assessment, the
knowledge of the explosive characteristics of the powder
(usually summarized in a few parameters, such as the
deflagration index (K_{St}), the lower explosive limit (LEL), the
minimum ignition energy (MIE), etc.) is of paramount
importance to provide an extent of the probability of
occurrence of a dust explosion.⁹ Such explosive parameters
for a given dust are usually estimated by experimental tests,
therefore requiring high costs and long times. Moreover, it is
quite cumbersome to test all the different particle size
distributions that can be present in a real plant where several

Special Issue: Giuseppe Storti Festschrift

Received: January 21, 2021

Revised: March 21, 2021

Accepted: March 26, 2021

65 unit operations (e.g., milling, granulation, etc.) are usually
66 involved. This is the reason because some predictive
67 mathematical models have been recently proposed in the
68 literature for estimating some of these explosive param-
69 eters.^{10–12}

70 Concerning the estimation of the MIE, some predictive
71 methods based on both group contribution models¹³ and
72 hybridization of gravitational search algorithm (GSA) with
73 support vector regression (SVR), using relatively few
74 descriptors (which include the number of carbon and
75 hydrogen atoms, as well as molecular weight of the
76 compound),¹⁴ have been successively applied to gaseous
77 compounds. Unfortunately, such models cannot be applied to
78 organic dusts, because they do not take into account for the
79 granulometric distribution of the powder, which is one the
80 most influencing factors for the estimation of MIE.¹⁵ The
81 importance of the granulometric distribution is so relevant that
82 several correlations for MIE determination as a function of
83 different granulometric distribution of either the same powder
84 or mixtures can be found in the current literature.^{16–18}

85 Recently, Hosseinzadeh et al.¹⁹ proposed a simple
86 mathematical model based on the heating of a dust particle
87 due to the energy spark in a Hartmann tube. Such a model
88 estimates the MIE as the smallest value of energy spark at
89 which the maximum temperature of the dust particle is equal
90 to the ignition temperature of the particle in a dust cloud, such
91 as that determined in a standard BAM oven, which can be
92 considered, in some way, an experimental information
93 equivalent to MIE.

94 The main aim of this work is to develop a simple
95 mathematical model able to theoretically estimate the MIE
96 of organic powders using very few easily accessible
97 experimental information, such as granulometric analysis and
98 thermogravimetric analysis (TGA). Particularly, TGA is used
99 to determine the pyrolysis kinetics of the dust, which is then
100 used within the model to compute the rate of combustible
101 volatiles released by the dust particles.

2. METHODS AND MATERIALS

102 **2.1. The Hartmann Tube Test.** The MIE is usually
103 determined using the Hartmann tube equipment, according to
104 different standard procedures; in particular, in this work we
105 refer to the standard procedure EN ISO/IEC 80079-20-
106 2:2016.²⁰

107 Accordingly, the electrical spark generated between the two
108 electrodes interacts with the dust dispersed in air inside the
109 Hartmann tube for a very short period. During this period, all
110 the processes of heat transfer from the spark to the flammable
111 air-dust mixture occur.

112 According to Sankhé et al. (2019),²¹ the spark between the
113 electrodes has a total duration of $\sim 100 \mu\text{s}$, and its
114 extinguishing phase is characterized by an almost spherical
115 distribution of the plasma around the electrodes. The complete
116 extinction of the effects due to the spark lasts for $\sim 240 \mu\text{s}$
117 beyond the end of the spark itself, and, at 1 ms, the
118 phenomenon is definitively expired. During this period, the
119 corona discharge fully develops, leading to high temperatures
120 of the small air volume between the electrodes.

121 The basic idea of this work is that a spark with a given
122 energy can ignite an air–dust mixture in the Hartmann tube
123 test only if the discharged energy is able to heat-up the small
124 volume of air near the electrodes above a threshold value.

Regardless how finding such a threshold value for a given
125 dust (this will be discussed later), we must first estimate an
126 effective value for such an air temperature, as a function of the
127 discharged energy in the Hartmann tube test.
128

129 Temperature and size of the hot region of quasi-spherical
130 shape (the so-called “hot core”) around the electrodes, as a
131 function of the energy content of the spark, can be visualized
132 during a test into the Hartmann tube using a high-frequency
133 thermocamera, as discussed by Bu et al. (2019).²² In this
134 paper, several photographs show, for different dusts and
135 different spark energy values, the time evolution of the quasi-
136 spherical region around the electrodes.

137 In particular, from such photographs, the size of the hot core
138 at a time equal to 0 [ms] is of interest in this work, since it can
139 be ascribed to the spark only and not to the subsequent
140 combustion phenomena. Actually, the pyrolysis of an organic
141 dust cannot start before $\sim 5\text{--}10$ ms, since such a time is
142 necessary to heat the combustible dust particles to temperature
143 values at which the devolatilization rate is not negligible.²²
144 While the dust particles are heated, flammable volatiles from
145 the dust pyrolysis mix with the surrounding air and they
146 possibly start a homogeneous combustion if the mixture of
147 flammable volatiles and air is within the flammability limits of
148 volatiles.

149 Therefore, analyzing the images of the hot zone in
150 correspondence of time equal to 0 ms, we have estimated
151 the size of the hot core as a function of the spark energy

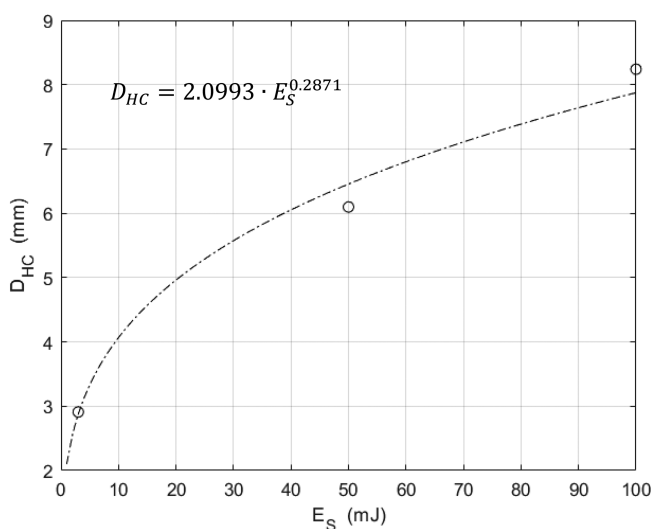


Figure 1. Equivalent diameter of the hot core, as a function of spark energy. Data derived from images reported in Bu et al. (2019).²²

content, as summarized in Figure 1. The following relation,
also reported in Figure 1, can represent these data by

$$D_{HC} = 2.0993 E_S^{0.2871} \quad (1)$$

where E_S indicates the energy content of the spark [mJ], and
 D_{HC} represents the equivalent diameter of the hot core [mm].
Note that this relationship is obviously reliable only in the
range of 3–100 mJ. Extrapolation to 1 mJ can be done with
reasonable confidence, since the relationship goes to zero at
the limit of $E_S = 0$; otherwise, extrapolation of spark energies
above 100 mJ are highly discouraged.

162 From this relationship, the effective temperature of the air in
163 the hot core can be estimated (as an order of magnitude) by
164 assuming that all the spark energy leads to an increase in the
165 enthalpy content of such air, that is $m \cdot C_p \cdot (T_{\text{air}} - T_{\text{amb}}) = E_s$.

166 Here, m is the mass of air in the hot core ($m = \left(\frac{\pi D_{\text{HC}}^3}{6}\right) \rho_{\text{air}}$), C_p
167 the specific heat at a constant pressure of air, T_{air} the effective
168 temperature of the air in the hot core, and T_{amb} the ambient air
169 temperature.

170 From such a relationship, together with eq 1, a relationsip
171 between T_{air} and E_s can be finally obtained:

$$T_{\text{air}} = T_{\text{amb}} + \frac{E_s}{\left(\frac{\pi D_{\text{HC}}^3}{6}\right) \rho_{\text{air}} C_p} \quad (2)$$

173 2.2. Mathematical Model for Particle Heating and

174 **Devolatilization.** As previously mentioned, the basic idea of
175 this work is to assume that the ignition spark creates a hot core
176 of air able to heat up the embedded dust particles, possibly
177 leading to their pyrolysis, and therefore to the emission of
178 flammable volatile gases. Only when mixing such flammable
179 volatile gases with the air in the hot core, leading to a mixture
180 composition within the flammability range, can a homoge-
181 neous combustion start, therefore triggering the dust explosion.

182 While the air temperature in the hot core following a spark
183 discharge with a given energy can be estimated as discussed in
184 the previous section, the estimation of the volatiles–air
185 composition requires modeling the heating, pyrolysis, and
186 volatile emission from a particle dust surrounded by the air in
187 the hot core. This has been done through a mathematical
188 model derived from a literature one developed for the
189 prediction of the deflagration index of organic dusts.¹¹ Such
190 a comprehensive model involves a pyrolysis phase incorporat-
191 ing a single devolatilization step, which converts the solid to
192 volatile compounds and a carbon residue called a “skeleton”.
193 All the parameters needed for such a pyrolysis model can be
194 derived from simple TGA.²³

195 The material and energy balance equations used to model
196 the particle heating and devolatilization are based on the
197 following hypotheses:¹¹ one-dimensional spherically symmetric
198 dust particle; negligible resistance to mass transfer and
199 negligible diffusive flux, with respect to the convective one
200 for the gas phase; no secondary reactions of the volatile
201 pyrolysis products; local thermal equilibrium between solid
202 and volatiles; constant heat capacity of the solid phase much
203 larger than that of the gaseous phase; constant temperature of
204 the air in the hot core region; pseudo-steady-state assumption
205 for the gas phase; particles with constant volume, V_t .

206 **Material Balance for the Solid Phase.** Having assumed the
207 presence of a solid residue after the pyrolysis, not all the mass
208 of the particle leads the volatile compound; therefore, the
209 material balance equation has been written only for the solid
210 fraction consumed by the pyrolysis reaction ($m_{S,r}$), as follows:

$$\frac{\partial m_{S,r}}{\partial t} = -r_p \cdot V_t = -k \cdot \rho_{S,r}^n \cdot V_t \quad (3)$$

212 Here, $\rho_{S,r}$ is the reactive mass per unit particle volume, defined
213 as

$$\rho_{S,r} = \frac{m_{S,r}}{V_t} = \frac{m_S}{V_t} - \frac{m_{S,0}}{V_t}$$

and β is the mass fraction of the particle leading to the
214 skeleton: 215

$$\beta = \frac{m_{S,f}}{m_{S,0}}$$

This value can be easily derived from TGA. In this definition,
216 $m_{S,0}$ is the initial mass of the solid, while $m_{S,f}$ is the skeleton
217 mass. 218

By also defining the term $\rho_{S,\text{app}}$, which is given as 219

$$\rho_{S,\text{app}} = \frac{m_S}{V_t} = \rho_S \cdot (1 - \varepsilon)$$

where ε is the porosity of the dust particle, 220

$$\varepsilon = \frac{V_t - V_S}{V_t} = \frac{V_V}{V_t}$$

and using the relation $\rho_{S,\text{app},0} = \frac{m_{S,0}}{V_t} = \rho_S \cdot (1 - \varepsilon_0) \approx \rho$, we can
221 derive the following expression: 222

$$\rho_{S,r} = \rho_{S,\text{app}} - \rho_{S,\text{app},0} \cdot \beta \quad (4) \quad 223$$

Using these expressions, eq 3 leads to the following equation
224 with the relative initial conditions: 225

$$\begin{cases} \frac{\partial \rho_{S,r}}{\partial t} = -k \cdot \rho_{S,r}^n \\ \text{I.C.: } \rho_{S,r}(t=0) = \rho_{S,r,0} = \rho_{S,\text{app},0} (1 - \beta) \end{cases} \quad (5) \quad 226$$

This equation can be made dimensionless by defining the
227 dimensionless particle density, 228

$$c_S = \frac{\rho_{S,r}}{\rho_{S,r,0}} = \frac{\rho_{S,r}}{\rho_{S,\text{app},0} (1 - \beta)}$$

as 229

$$\begin{cases} \frac{\partial c_S}{\partial t} = -k \cdot \rho_{S,r,0}^{n-1} \cdot c_S^n \\ \text{I.C.: } c_S(t=0) = 1 \end{cases} \quad (6) \quad 230$$

The kinetic constant, k , can be represented by a modified
231 Arrhenius equation, whose parameters can be also derived
232 from TGA.²³ 233

$$k = A \exp\left[-\frac{E_a(1 - \chi\alpha)}{RT}\right] \quad (7) \quad 234$$

where χ accounts for the dependence of the activation energy
235 on the particle conversion α , 236

$$\alpha = \frac{m_{S,r,0} - m_{S,r}}{m_{S,r,0}} = 1 - c_S$$

This leads to the following final form of the material balance
237 for the solid phase: 238

$$\begin{cases} \frac{\partial c_S}{\partial t} = -A \exp\left[-\frac{E_a[1 - \chi(1 - c_S)]}{RT}\right] \rho_{S,r,0}^{n-1} c_S^n \\ \text{I.C.: } c_S(t=0) = 1 \end{cases} \quad (8) \quad 239$$

Particle Material Balance for the Volatiles. By defining the
240 apparent volatile density, $\rho_{V,\text{app}}$, as 241

$$\rho_{V,\text{app}} = \frac{m_V}{V_t} = \frac{m_V}{V_V} \cdot \frac{V_V}{V_t} = \rho_V \cdot \varepsilon$$

242 thanks to the pseudo-steady-state assumption, the particle
243 material balance for the volatiles in spherical coordinates leads
244 to the following expression:

$$\frac{\partial(v_x \rho_V \varepsilon)}{\partial r} = -\frac{2}{r}(v_x \rho_V \varepsilon) + k \rho_{S,r}^n \quad (9)$$

246 Introducing the new variables $v = \rho_V \cdot \varepsilon \cdot v_x$ (which represents
247 the massive rate of volatile gases exiting from the external
248 surface of a single dust particle per unit particle surface)
249 together with its ratio to $\rho_{S,r,0}$

$$V = \frac{v}{\rho_{S,r,0}}$$

250 the final form of the material balance for the volatiles with the
251 relative boundary condition can be obtained:

$$\left\{ \begin{array}{l} \frac{\partial V}{\partial r} = -\frac{2}{r}V + k \rho_{S,r,0}^{n-1} c_S^n \\ \text{B.C.: } V(r=0) = 0 \end{array} \right. \quad (10)$$

253 **Particle Energy Balance.** The energy balance equation for
254 the particle can be written as

$$\rho_{S,\text{eff}} c_{p,S} \frac{\partial T}{\partial t} = -\nabla \times (h \cdot \vec{v} + \vec{q}) - \Delta H_{\text{pyr}} k \rho_{S,r}^n \quad (11)$$

256 where $\rho_{S,\text{eff}} = \rho_S(1 - \bar{\varepsilon})$ is the effective particle density, using
257 an effective average value of $\bar{\varepsilon} = 0.5$; $h = \rho_{V,\text{app}} c_{p,V} T$ is the
258 enthalpy of the volatiles per unit of volume; $\vec{q} = -\bar{\lambda} \cdot \nabla T$ is
259 the conductive heat flux, $\bar{\lambda} = \lambda \cdot (1 - \bar{\varepsilon})$ representing the
260 effective thermal conductivity; ΔH_{pyr} is the endothermic
261 reaction enthalpy for the pyrolysis reaction. Using these
262 definitions, the previous equation can be recast in the following
263 one, with the relative boundary and initial conditions:

$$\left\{ \begin{array}{l} \rho_S \cdot (1 - \bar{\varepsilon}) \cdot c_{p,S} \frac{\partial T}{\partial t} = \bar{\lambda} \cdot \frac{\partial^2 T}{\partial r^2} + \frac{2}{r} \bar{\lambda} \cdot \frac{\partial T}{\partial r} \\ \quad - c_{p,V} \cdot \left[\frac{\partial}{\partial r}(v \cdot T) + \frac{2}{r} \cdot (v \cdot T) \right] - \Delta H_{\text{pyr}} k \rho_{S,r}^n \\ \text{I.C.: } T(t=0) = T_0 \\ \text{B.C.: } \left\{ \begin{array}{l} \bar{\lambda} \cdot \frac{\partial T}{\partial r} \Big|_{r=0} = 0 \\ \bar{\lambda} \cdot \frac{\partial T}{\partial r} \Big|_{r=R} = -h_c \cdot (T|_{r=R} - T_{\text{air}}) - \varepsilon_{\text{em}} \cdot \sigma \cdot (T|_{r=R}^4 - T_{\text{air}}^4) \end{array} \right. \end{array} \right. \quad (12)$$

265 where h_c is the heat-transfer coefficient, ε_{em} is the emissivity of
266 the dust (assumed equal to 0.95), and σ is the Stefan–
267 Boltzmann constant.

268 Note that the BCs of this equation involve the temperature
269 of the air surrounding the dust particle, that is, the temperature
270 of the hot core created by the ignition spark. This value can be
271 estimated, for a given spark energy, as discussed in the previous
272 section.

273 It is possible to rewrite this equation by introducing the
274 previous dimensionless variables, as follows:

$$\left\{ \begin{array}{l} \frac{\partial T}{\partial t} = \frac{\lambda}{\rho_S \cdot c_{p,S}} \left(\frac{\partial^2 T}{\partial r^2} + \frac{2}{r} \frac{\partial T}{\partial r} \right) - \frac{(1 - \beta) \cdot c_{p,V}}{(1 - \bar{\varepsilon}) \cdot c_{p,S}} \\ \quad \cdot \left[\frac{\partial V}{\partial r} \cdot T + V \cdot \frac{\partial T}{\partial r} + \frac{2}{r} \cdot (V \cdot T) \right] - \frac{\Delta H_{\text{pyr}} \cdot (1 - \beta)}{(1 - \bar{\varepsilon}) \cdot c_{p,S}} \\ \quad \cdot k \cdot \rho_{S,r,0}^{n-1} \cdot c_S^n \\ \text{I.C.: } T(t=0) = T_0 \\ \text{B.C.: } \left\{ \begin{array}{l} \left. \frac{\lambda}{\rho_S \cdot c_{p,S}} \cdot \frac{\partial T}{\partial r} \right|_{r=0} = 0 \\ \left. \frac{\lambda}{\rho_S \cdot c_{p,S}} \cdot \frac{\partial T}{\partial r} \right|_{r=R} = -\frac{h_c}{\rho_S \cdot (1 - \bar{\varepsilon}) \cdot c_{p,S}} \cdot (T|_{r=R} - T_{\text{air}}) \\ \quad - \frac{\varepsilon_{\text{em}} \cdot \sigma}{\rho_S \cdot (1 - \bar{\varepsilon}) \cdot c_{p,S}} \cdot (T|_{r=R}^4 - T_{\text{air}}^4) \end{array} \right. \end{array} \right. \quad (13) \quad 275$$

Material Balance for the Volatiles in the Hot Core. To
276 know whether the concentration of the volatile gases in the hot
277 core reaches the lower flammability limit (LFL) or not during
278 the dust particle heating and devolatilization, the material
279 balance equation for the volatiles in the hot core is required.

The massive rate of volatile gases leaving a single dust
281 particle (and therefore entering the surrounding air in the hot
282 core, possibly forming a flammable mixture) per unit area at
283 each moment is equal to the value of v at the outer edge of the
284 particle, that is, $\rho_{S,r,0} \cdot V(r=R, t)$. Therefore, the total mass rate
285 of volatiles entering the hot core can be computed as
286

$$\dot{m}_V(t) = \rho_{S,r,0} V(r=R, t) \pi D_p^2 N_p \quad (14) \quad 287$$

where D_p is the particle average diameter (e.g., the D_{50} value
288 computed from the particle size distribution of the dust); $N_p =$
289 $\frac{C_p V_{\text{HC}}}{m_p}$ (where C_p is the dust concentration in the hot core, V_{HC}
290 is the hot core volume, and m_p is the mass of a single particle)
291 is the number of solid particles within the hot core. The dust
292 concentration in hot core has been estimated by assuming that
293 the dust loaded in the Hartmann tube uniformly distribute in
294 two-thirds of the volume of the Hartmann tube.
295

Therefore, the material balance equation for the volatiles in
296 the hot core becomes
297

$$\frac{d m_V}{d t} = \dot{m}_V \quad (15) \quad 298$$

Introducing the volatile concentration ρ_V , which is defined as
299

$$\rho_V = \frac{m_V}{V_{\text{HC}}}$$

together with eq 14, the previous equation leads to the
300 following equation with the relative initial conditions:
301

$$\left\{ \begin{array}{l} \frac{d \rho_V}{d t} = \frac{\rho_{S,r,0} \cdot V(r=R, t) \pi D_p^2 N_p}{V_{\text{HC}}} \\ \text{I.C.: } \rho_V(t=0) = 0 \end{array} \right. \quad (16) \quad 302$$

Equations 8, 10, 13, and 16 constitute a mixed system of
303 ordinary and partial differential equations that, once numeri-
304 cally integrated, gives the space and time evolution of $c_S(r, t)$,
305 $V(r, t)$, $T(r, t)$, and $\rho_V(t)$. The integration has been performed
306 through the Method of Lines,²⁴ with the spatial derivatives
307

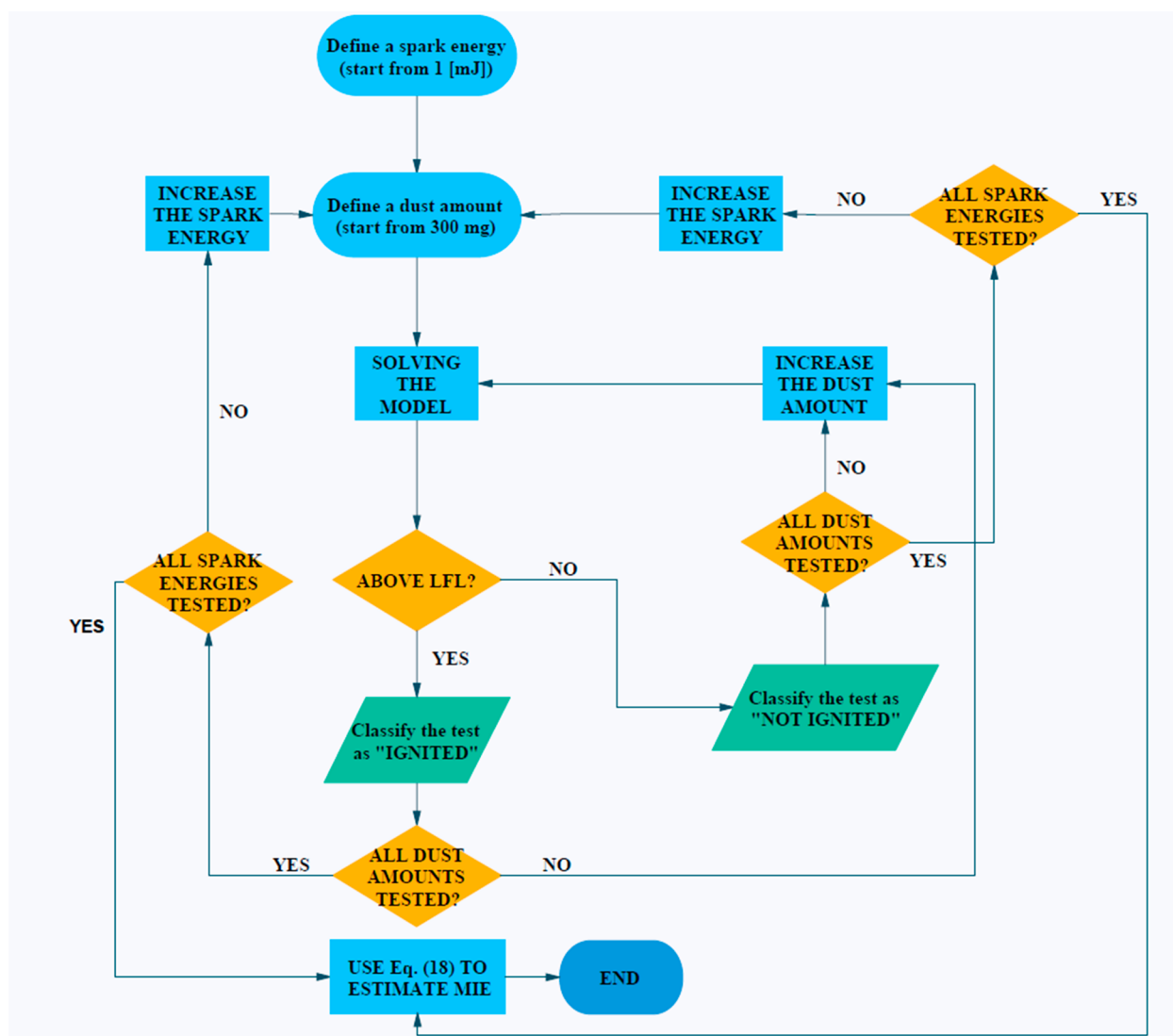


Figure 2. Flowchart of the proposed MIE estimation procedure.

308 approximated using a constant step, five-point centered finite
309 difference scheme.²⁵

310 In particular, during the integration of the system of
311 equations for a given dust ignited by a spark with a given
312 energy, the time evolution of the volatile concentration in the
313 hot core region is computed. If such a concentration reaches
314 (in a reasonable small time, for example, <120 ms) the lower
315 flammability limit of the volatile gases, a homogeneous
316 combustion can be triggered, finally leading to the dust
317 explosion.

3. MIE ESTIMATION PROCEDURE

318 The evidence derived from the Hartmann tube experiments,
319 together with the mathematical modeling of the dust particles
320 heating and devolatilization, for a given dust ignited by a spark
321 with a given energy, allow one to estimate the volatile
322 concentration in the hot core region. If such a concentration
323 reaches the LFL of the volatiles within 120 ms, we assume that
324 the dust is ignited.

325 However, this first requires the definition of the LFL of the
326 volatile gases produced during the dust pyrolysis. This is not a
327 simple task, since different flammable gases can be emitted

during the dust pyrolysis, possibly also changing the
composition with temperature. To simplify this rough
problem, it is reasonable to assume that when polymer dusts
are involved, their monomers are representative of the
flammability properties of the volatile gases produced, whereas,
for all of the other organic dusts, methane is the species that
can effectively represent the flammable properties of the
volatile gases. Therefore, the LFL of the monomers (in
particular, 0.9% [v/v] at 25 °C for styrene) and methane
(4.95% [v/v] at 25 °C) were used in the following
computations, after correcting them for the temperature
influence according to eq 17.²⁶

$$\text{LFL} = \text{LFL}_{25} - \frac{100c_{p,L}}{\Delta H_c}(T - 25) \quad (17)$$

341 Since this work aims to estimate the MIE values as
342 experimentally measured in the Hartmann tube test, the
343 experimental procedure detailed in the standard EN ISO/IEC
344 80079-20-2:2016²⁰ must be reproduced. In particular, this
345 standard requires that several amounts of dust (namely, 300,
346 600, 900, 1200, and 1500 mg) must be loaded to the
347 Hartmann tube and each of them must be ignited by a spark

with increasing energy (namely, 1, 3, 10, 30, 100, 300, and 1000 mJ) until the dust ignition is detected. The MIE value can be then statistically calculated using the following expression:²²

$$\text{MIE} = 10^{[\log_{10}(E2) - I(E2) \cdot (\log_{10}(E2) - \log_{10}(E1))] / ([NI + I](E2) + 1)} \quad (18)$$

where E2 is the minimum energy at which at least one of the dust amounts is ignited, E1 the maximum energy at which the ignition of all the dust amounts always fail, I(E2) the number of dust amounts ignited at energy E2, and [NI + I](E2) the total number of tests (resulting in both dust ignition and dust not ignition) performed at the energy E2.

Therefore, the procedure proposed for the estimation of the MIE of a given dust is summarized in both the following algorithm and the flowchart of Figure 2.

- (1) Define the spark energy (inside the reliability range of eq 1, therefore starting from 1 mJ).
- (2) Define the dust amount (starting from 300 mg).
- (3) Compute the hot core equivalent diameter through eq 1 and the corresponding effective air temperature through eq 2.
- (4) Integrate eqs 8, 10, 13, and 16 from 0 to 120 ms and compare the computed values of ρ_V (suitably transformed in units % (v/v)) to the corresponding LFL value at the air temperature calculated from eq 2.
- (5) If the concentration of the volatiles gases reaches the LFL value within 120 ms, the test is classified as “ignited”; otherwise, it is classified as “not ignited”.
- (6) Regardless of the test result, increase the dust amount to the following value and go back to step 3 until the last dust amount value is reached; then, increase the spark energy and repeat the procedure from step 2 onward, until the last spark energy to be verified.
- (7) Compute the MIE value using eq 18.

4. RESULTS AND DISCUSSION

The proposed procedure for the estimation of the MIE was validated with comparison to the experimental results of seven different organic powders, namely, acid acetylsalicylic, cork, corn starch, niacin, polystyrene, sugar, and wheat flour.

The procedure requires the values of several parameters for each dust, such as chemical–physical parameters, kinetic parameters, and geometric parameters. While all the chemical–physical and kinetic parameters are summarized in a previous work¹¹ to which the reader is referred to, the geometric and explosibility characteristics of the considered powders are summarized in Table 1.

The results obtained with the proposed procedure are summarized in Table 2 (in terms of E1 and E2 values, together with the corresponding I and NI values and the MIE value computed through eq 17 and in Figure 3, in terms of parity plot of experimental and estimated values.

From the parity plot of Figure 3, it is possible to notice that almost all the predicted MIE values are close or inside $\pm 50\%$ boundaries, therefore supporting the reliability of the proposed approach.

5. CONCLUSIONS

The main aim of this work was to develop a simple procedure for the estimation of the MIE of organic dusts based on

Table 1. D_{50} , Lower Flammability Limits (LFLs) at 25 °C,^a and Experimental MIE Values^{b,c}

	D_{50} [μm]	LFL ₂₅ [% v/v]	MIE _{EXP} [mJ]
acid acetylsalicylic	39	4.95	1
cork	17	4.95	3
corn starch	12	4.95	30
	74	4.95	88
niacin	15	4.95	1
polystyrene	40	0.90	10
sugar	34	4.95	10
wheat flour	52	4.95	30

^aTo be used for the LFL determination at a given temperature. ^bIn the case of a range of MIE, the lowest value is reported. ^cData values taken from refs 22 and 27–29.

Table 2. Results for the Predicted MIE Values

spark energy	300 mg	600 mg	900 mg	1200 mg	1500 mg	$P = I / (I + NI)$
Acid Acetylsalicylic: MIE_{PRED} = 1						
1	I	I	I	I	I	5/5
0	NI	NI	NI	NI	NI	0/5
Sugar: MIE_{PRED} = 6						
10	NI	NI	I	I	I	3/5
3	NI	NI	NI	NI	NI	0/5
Wheat Flour: MIE_{PRED} = 17						
30	NI	NI	I	I	I	3/5
10	NI	NI	NI	NI	NI	0/5
Cork: MIE_{PRED} = 5						
10	NI	I	I	I	I	4/5
3	NI	NI	NI	NI	NI	0/5
Corn Starch ($D_{50} = 12 \mu\text{m}$): MIE_{PRED} = 13						
30	I	I	I	I	I	5/5
10	NI	NI	NI	NI	NI	0/5
Corn Starch ($D_{50} = 74 \mu\text{m}$): MIE_{PRED} = 55						
100	NI	NI	I	I	I	3/5
30	NI	NI	NI	NI	NI	0/5
Polystyrene: MIE_{PRED} = 55						
100	NI	NI	I	I	I	3/5
30	NI	NI	NI	NI	NI	0/5
Niacin: MIE_{PRED} = 1						
1	I	I	I	I	I	5/5
0	NI	NI	NI	NI	NI	0/5

accessible physicochemical properties and lumped devolatilization kinetics parameters easily obtained from simple TGA.

The procedure simulates the ignition phenomenon that occurs inside the Hartmann tube, which is the equipment most frequently used for the experimental determination of MIE, by assuming that the ignition spark suddenly heats up the air in a small volume near the electrodes, which then leads to the heating and devolatilization of the dust particles. When such a devolatilization is able to create a flammable gas mixture in the small region close to the electrodes, the dust is assumed to ignite.

The proposed procedure was validated by comparing the predicted MIE values with the experimental ones for seven organic powders: acid acetylsalicylic, cork, corn starch, niacin, polystyrene, wheat flour, and sugar. The proposed procedure allowed estimation of the values of MIE for the different organic dusts with an encouraging accuracy; indeed, the results achieved are promising and could constitute the basis for future implementation of the proposed procedure, which

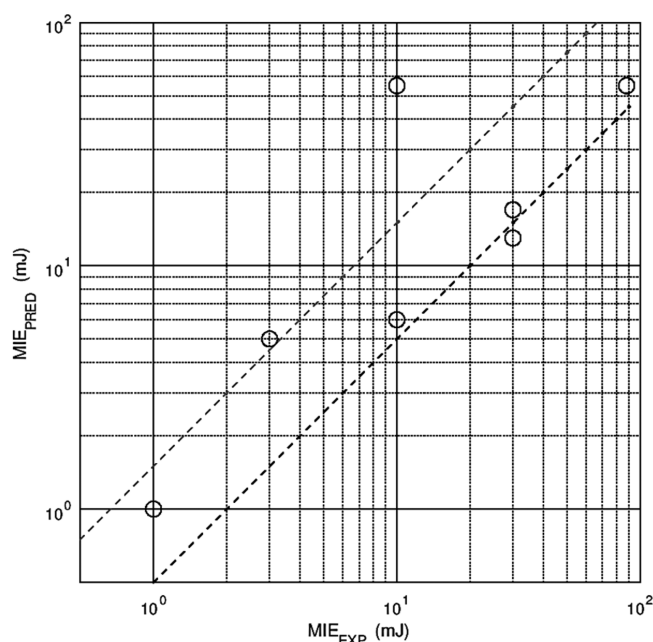


Figure 3. Comparison among predicted and experimental values of MIE. Dashed lines represent $\pm 50\%$ boundaries.

422 obviously must be further validated, independently, against a
423 wider set of organic dusts.

424 Even if the experimental measure of MIE remains the safest
425 and most accurate method for its determination, after a more
426 complete validation, the proposed procedure could accelerate
427 the risk analysis concerning dust explosion and, consequently,
428 increase the safety related to both the processing and storage of
429 potentially explosive powders.

430 AUTHOR INFORMATION

431 Corresponding Author

432 **Renato Rota** – Dip. di Chimica, Materiali e Ingegneria
433 Chimica “G. Natta”, Politecnico di Milano, 20131 Milano,
434 Italy; orcid.org/0000-0002-3253-4424;
435 Email: renato.rota@polimi.it

436 Authors

437 **Sabrina Copelli** – Dipartimento di Scienza e Alta Tecnologia
438 (DISAT), Università degli Studi dell’Insubria, 21100 Varese,
439 Italy

440 **Martina S. Scotton** – Dipartimento di Scienza e Alta
441 Tecnologia (DISAT), Università degli Studi dell’Insubria,
442 21100 Varese, Italy

443 **Marco Barozzi** – Dipartimento di Scienza e Alta Tecnologia
444 (DISAT), Università degli Studi dell’Insubria, 21100 Varese,
445 Italy

446 **Marco Derudi** – Dip. di Chimica, Materiali e Ingegneria
447 Chimica “G. Natta”, Politecnico di Milano, 20131 Milano,
448 Italy

449 Complete contact information is available at:

450 <https://pubs.acs.org/10.1021/acs.iecr.1c00309>

451 Notes

452 The authors declare no competing financial interest.

453 REFERENCES

454 (1) Increase in process safety incidents post-lockdown; available via
455 the Internet at: <https://www.ioshmagazine.com/2020/08/04/>

increase-process-safety-incidents-post-lockdown (last accessed Jan. 20, 2021).

(2) Industrial Union; available via the Internet at: <http://www.industrialunion.org/indias-safety-crisis-industrial-accidents-during-covid-19-kill-at-least-75> (last accessed Jan. 20, 2021).

(3) Role of Operations and Maintenance in Process Safety Management. In *Guidelines for Safe Process Operations and Maintenance*; John Wiley & Sons, Ltd., 1995; pp 11–31.

(4) Beirut Explosion: What We Know So Far. *BBC News*. Aug. 11, 2020.

(5) Cloney, C. 2019—Dust Safety Science—Combustible Dust Incident Report, 2019.

(6) Cloney, C. 2020—Dust Safety Science—Mid Year Combustible Dust Incident Report, 2020.

(7) Barozzi, M.; Copelli, S.; Scotton, M. S.; Torretta, V. Application of an Enhanced Version of Recursive Operability Analysis for Combustible Dusts Risk Assessment. *Int. J. Environ. Res. Public Health* **2020**, *17* (9), 3078.

(8) Barozzi, M.; Scotton, M. S.; Derudi, M.; Copelli, S. Recursive operability analysis as a tool for risk assessment in plants managing metal dusts. *Chem. Eng. Trans.* **2020**, *82*, 43–48.

(9) Hassan, J.; Khan, F.; Amyotte, P.; Ferdous, R. A model to assess dust explosion occurrence probability. *J. Hazard. Mater.* **2014**, *268*, 140–149.

(10) Fumagalli, A.; Derudi, M.; Rota, R.; Copelli, S. Estimation of the Deflagration Index K_{St} for Dust Explosions: A Review. *J. Loss Prev. Process Ind.* **2016**, *44*, 311–322.

(11) Copelli, S.; Barozzi, M.; Scotton, M. S.; Fumagalli, A.; Derudi, M.; Rota, R. A Predictive Model for the Estimation of the Deflagration Index of Organic Dusts. *Process Saf. Environ. Prot.* **2019**, *126*, 329–338.

(12) Scotton, M. S.; Barozzi, M.; Derudi, M.; Rota, R.; Copelli, S. Kinetic Free Mathematical Model for the Prediction of K_{St} Values for Organic Dusts with Arbitrary Particle Size Distribution. *J. Loss Prev. Process Ind.* **2020**, *67*, 104218.

(13) Eini, S.; Jhamb, S.; Sharifzadeh, M.; Rashtchian, D.; Kontogeorgis, G. M. Developing group contribution models for the estimation of Atmospheric Lifetime and Minimum Ignition Energy. *Chem. Eng. Sci.* **2020**, *226*, 115866.

(14) Owolabi, T. O.; Suleiman, M. A.; Adeyemo, H. B.; Akande, K. O.; Alhiyafi, J.; Olatunji, S. O. Estimation of minimum ignition energy of explosive chemicals using gravitational search algorithm based support vector regression. *J. Loss Prev. Process Ind.* **2019**, *57*, 156–163.

(15) Castellanos, D.; Bagaria, P.; Mashuga, C. V. Effect of particle size polydispersity on dust cloud minimum ignition energy. *Powder Technol.* **2020**, *367*, 782–787.

(16) Bisel, A.; Kubainsky, C.; Steiner, D.; Bordeaux, D.; Benabdillah, J. The minimum ignition energy of powder mixtures. *Chem. Eng. Trans.* **2016**, *48*, 433–438.

(17) Hosseinzadeh, S.; Norman, F.; Verplaetsen, F.; Berghmans, J.; Van den Bulck, E. Minimum ignition energy of mixtures of combustible dusts. *J. Loss Prev. Process Ind.* **2015**, *36*, 92–97.

(18) Zhang, X.; Shen, Q.; Shen, X.; Zhang, Z.; Xu, S.; Ye, S. Minimum ignition energy of medicinal powder - Florfenicol and Tilmicosin. *J. Loss Prev. Process Ind.* **2016**, *39*, 30–38.

(19) Hosseinzadeh, S.; Berghmans, J.; Degreve, J.; Verplaetsen, F. A model for the minimum ignition energy of dust clouds. *Process Saf. Environ. Prot.* **2019**, *121*, 43–49.

(20) EN ISO/IEC 80079-20-2:2016, Explosive atmospheres—Part 20-2: Material characteristics—Combustible dusts test methods.

(21) Sankhé, M.; Bernard, S.; Wartel, M.; Pellerin, S.; Gillard, P. Characterization of a Spark Discharge for Dust Cloud Ignition. *Contrib. Plasma Phys.* **2019**, *59* (3), 326–339.

(22) Bu, Y.; Yuan, C.; Amyotte, P.; Li, C.; Cai, J.; Li, G. Ignition Hazard of Non-Metallic Dust Clouds Exposed to Hotspots versus Electrical Sparks. *J. Hazard. Mater.* **2019**, *365*, 895–904.

(23) Fumagalli, A.; Derudi, M.; Rota, R.; Snoeys, J.; Copelli, S. Prediction of K_{St} Reduction with the Particle Diameter Increase for Organic Dust. *J. Loss Prev. Process Ind.* **2017**, *50*, 67–74.

- 525 (24) Schiesser, W. *The Numerical Method of Lines*, 1st Edition;
526 Academic Press, 1991.
- 527 (25) Vande Wouwer, A.; Saucez, P.; Schiesser, W. E. Simulation of
528 Distributed Parameter Systems Using a Matlab-Based Method of
529 Lines Toolbox: Chemical Engineering Applications. *Ind. Eng. Chem.*
530 *Res.* **2004**, *43* (14), 3469–3477.
- 531 (26) Kondo, S.; Takizawa, K.; Takahashi, A.; Tokuhashi, K. On the
532 temperature dependence of flammability limits of gases. *J. Hazard.*
533 *Mater.* **2011**, *187* (1–3), 585–590.
- 534 (27) GESTIS-DUST-EX; available via the Internet at: [https://](https://staubex.ifa.dguv.de/?lang=e)
535 staubex.ifa.dguv.de/?lang=e (last accessed Jan. 18, 2021).
- 536 (28) Addai, E. K.; Gabel, D.; Kamal, M.; Krause, U. Minimum
537 ignition energy of hybrid mixtures of combustible dusts and gases.
538 *Process Saf. Environ. Prot.* **2016**, *102*, 503–512.
- 539 (29) NIOSH Pocket Guide to Chemical Hazards; available via the
540 Internet at: <https://www.cdc.gov/niosh/npg/npgd0571.html> (last
541 accessed March 21, 2021).